A New Sol–Gel Route for the Preparation of Nanometer-Scale Semiconductor Particles That Exhibit Quantum Optical Behavior

Yining Zhang,[†,‡] Narayan Raman,[‡,§] Joseph K. Bailey,[‡,§] C. Jeffrey Brinker,*[,‡,§] and Richard M. Crooks*[,†,‡]

Department of Chemistry and UNM/NSF Center for Micro-Engineered Ceramics, University of New Mexico, Albuquerque, New Mexico 87131, and Department 1846, Sandia National Laboratories, Albuquerque, New Mexico 87185 *(Received: August 6, 1992; In Final Form: September 15, 1992)*

A new sol-gel route for the preparation of nanometer-scale ZnS semiconductor particles that display quantum optical behavior is reported. Exploiting the scaling relationship between size and density of fractal polymeric precursors, films are prepared with narrow pore size distributions that serve as templates to constrain the growth of ZnS semiconductor particles. Blue shifts of the ZnS absorption threshold indicate that the particle size is reduced from 4.6 to 2.3 nm as the pore size is reduced from 3.5 to ≤2.0 nm. Results obtained using transmission electron microscopy are in general agreement with the spectroscopic results. This is a general approach for preparing thin-film nanocomposite materials with tailored optical and/or electronic properties.

Introduction

We wish to report a new sol–gel route for the synthesis of nanometer-scale semiconductor particles. The new aspects of our synthetic approach include the following: (1) the average particle size is correlated to the pore dimensions of the sol–gel–film host; (2) the particles are confined within an inert, ultrapure, inorganic glass matrix and are therefore stable and optically transparent; (3) since the films can be very thin, the particles may provide a quantum interface useful for certain types of technological devices; (4) the synthetic method is applicable to a range of metals and semiconductors; (5) the particles can be used as a direct probe of the pore structure of sol–gel-derived films.

Quantum particles (Q-particles) generally contain 10–500 subunits and are 1–10 nm in diameter. Since they are large enough to maintain bulk crystal structure, but too small to form continuous bands of electronic states, the electronic and optical properties of Q-particles differ from either molecules or bulk materials.[1-10] For example, Q-particles display optical behavior characterized by a continuous blue shift in the optical absorption threshold as their dimensions are reduced.

Previous studies have addressed the preparation of Q-particles in a variety of media, but it has proven difficult to control particle size and also obtain optical quality films.[4,11-28] In the present paper, we relate the pore volume of optical-quality, dip-coated, sol–gel-derived films to the size and distribution of ZnS Q-particles precipitated therein. There have been previous examples of Q-particle synthesis within glasses but not within films containing narrow pore size distributions. For example, glass films have been cast from binary sols containing both the host and the guest particles, but this method does not take maximum advantage of the film pore structure since the Q-particles define the pore size rather than vice versa.[26,27] Q-particles have also been formed in porous Vycor glass, but the pore size distribution is not well controlled in this medium.[28]

Experimental Section

Aluminoborosilicate polymers prepared from mixtures of the alkoxides by a sol–gel method[29] and characterized by a mass fractal dimension[30] $D \cong 2.4$ were aged from 0 to 14 days at 50 °C, causing their hydrodynamic radius, R, to vary from 3 to 19 nm.[30] Due to the scaling relationship of porosity and size of fractal objects ($\sim R^{(3-D)}$),[30] the degree of porosity and pore size of films prepared by dip-coating onto quartz glass substrates increases with aging time (Table I).[31,32] ZnS particles were synthesized within the pore network of the films by soaking in 0.1 M $(CH_3CO_2)_2Zn$ followed by dehydration and reaction with flowing H_2S gas at 100 °C for 1 h.

TABLE I: Relationship of Sol Aging Time to Median Pore Diameter and ZnS Particle Size

	sol aging time (days)		
	0	5	10
median pore diameter[a] (nm)	≤2.0[b]	3.1	3.5
pore volume[a] (%)	5[c]	19	29
ZnS particle diameter: UV–vis (nm)	2.3	4.0	4.6
ZnS particle diameter: TEM (nm)	<1.0[d]	2.3	2.5

[a] Determined by N_2 desorption isotherms acquired on films using a surface acoustic wave technique.[31,32] [b] Microporous film. [c] Determined from the refractive index using a Lorentz–Lorentz model and assuming a bulk refractive index of 1.48.[31] [d] TEM analysis showed no identifiable particles, although corresponding energy dispersive spectroscopy indicated the presence of Zn and S at low concentration.

A JEOL 2000FX STEM equipped with a Tracor-Northern EDS analyzer was used for particle imaging. TEM samples were prepared by scraping the composite film off the quartz substrate and onto carbon-coated TEM support grids. Electron diffraction and energy dispersive spectroscopy (EDS) were used to identify the ZnS phase particles. Dark-field imaging was performed using a 50-μm objective aperture centered over the (111) reflections of the ZnS sphalerite pattern.[33] Dark-field TEM images were used to measure particle size distributions. Micrographs were digitized with a resolution of 100 dots/in. The digitized images were analyzed by manually selecting the particles and measuring their areas and the major and minor axes of the smallest ellipse that contained them. When no noticeable drift had occurred during the exposure, the area of the particle was converted to a radius, assuming circular patterns. In micrographs where noticeable drift had occurred, the minor axis of the ellipse was used as the radius. All the particles in three micrographs, each from a different area of the sample, were analyzed.

Results and Discussion

The UV–vis spectra of ZnS Q-particles contained within the pores of sol–gel-derived films (Figure 1) indicate absorption thresholds at 280, 310, and 315 nm.[34] The blue shift of the threshold, relative to that of bulk-phase ZnS (Figure 1d), results from quantum confinement.[2,5,6,10] According to a tight binding calculation and the 350-nm absorption threshold for bulk-phase ZnS, the diameters of film-constrained Q-particles are 2.3, 4.0, and 4.6 nm for films prepared from sols aged at 50 °C for 0, 5, and 10 days, respectively.[3] The important point is that smaller pore sizes yield smaller Q-particle sizes, demonstrating that growth

* Authors to whom correspondence should be addressed.
† Department of Chemistry, University of New Mexico.
‡ UNM/NSF Center of Micro-Engineered Ceramics, University of New Mexico.
§ Sandia National Laboratories.

0022-3654/92/2096-9098$03.00/0

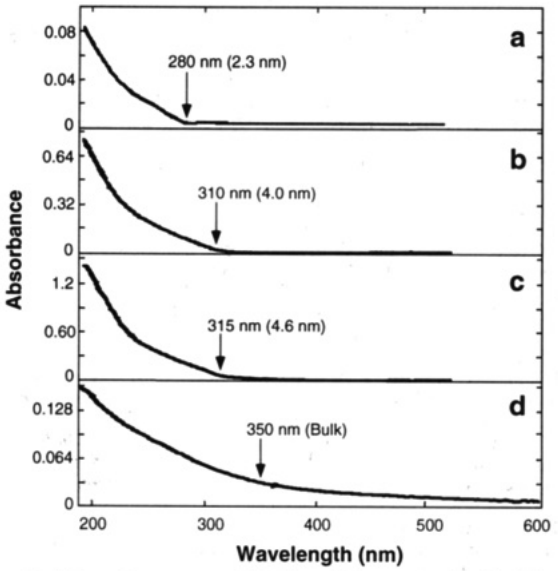

Figure 1. Absorption spectra of ZnS particles encapsulated within sol–gel-derived films prepared from aluminoborosilicate sols aged at 50 °C for (a) 0, (b) 5, and (c) 10 days. The arrows indicate the absorption thresholds used to obtain the particle diameters given in parentheses. (d) Absorption spectrum of bulk-phase ZnS.

of ZnS is constrained by the controlled pore size matrix. Films cast from sols aged for shorter times also have reduced volume fraction porosity (Table I) and therefore lower total absorption intensities.

A dark-field TEM micrograph of a ZnS composite film is shown in Figure 2. The film was prepared by reacting $(CH_3CO_2)_2Zn$ and H_2S at 100 °C within the pores of a film prepared from a sol aged for 10 days. The bright spots are crystalline ZnS particles which can be indexed as the sphalerite phase of ZnS by the three observable diffraction rings, which correspond to the (111), (220), and (311) reflections, shown in the lower inset of Figure 2. Image analysis indicates tht the particles are well dispersed throughout the gel matrix and that the number-average particle diameter is 2.5 nm (σ = 1.4 nm). In general, the particle sizes determined by TEM are about half those calculated from the absorption threshold (Table I). Since the model used to obtain the particle diameters may not be exactly appropriate for this system, and since the choice of the position of the absorption threshold is somewhat arbitrary, we view the agreement between these results as adequate. The important point is that the Q-particle sizes scale approximately linearly with the pore size of the dried gel films, demonstrating the templating function of the pores.

When the thin-film ZnS composites prepared from an unaged sol are annealed, we find a progressive red shift of the absorption threshold with increasing temperature (100–600 °C), consistent with a coarsening of the particle size. Annealing at 400 °C results in a mean particle diameter increase from 2.3 to 4.6 nm,[3] which is much larger than the dried gel film pore diameter, about 2 nm. This indicates that the pore walls do not effectively constrain particle growth under these conditions or that the ZnS particles become elongated in the unconstrained direction parallel to pore channels. Growth presumably occurs by a coarsening process driven by the difference in vapor pressure of the smallest and largest particles.[35] These results indicate that Q-particles may be useful as a probe of the sol–gel-derived film structure.

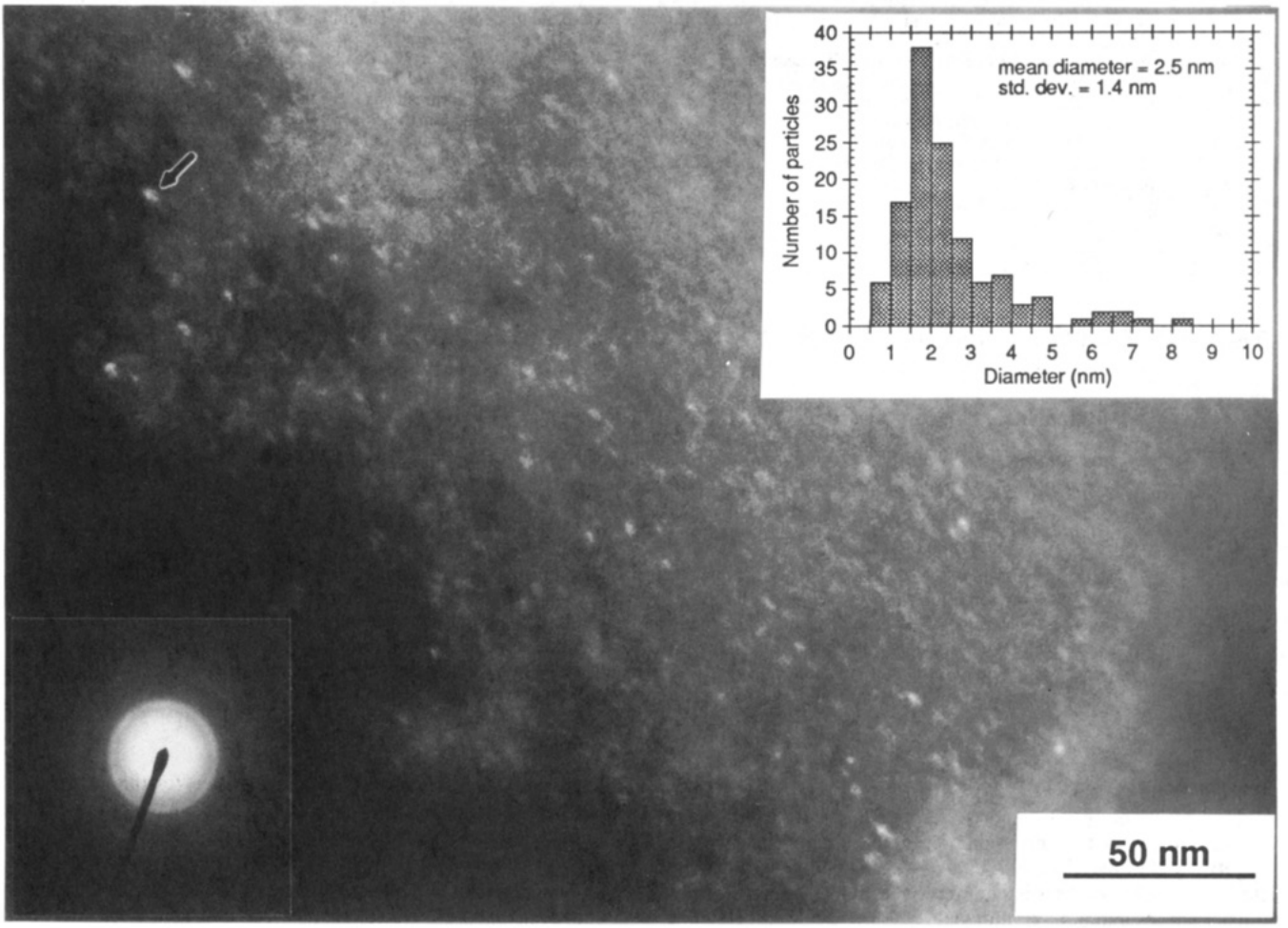

Figure 2. Dark-field TEM micrograph of a ZnS composite film prepared from a sol aged for 10 days. The bright spots are crystalline ZnS particles satisfying the (111) diffraction condition. The upper inset shows the number-average particle size distribution. The lower inset is a diffraction pattern that can be indexed as the sphalerite phase of ZnS by the three observable diffraction rings corresponding to the (111), (220), and (311) reflections. Corresponding energy dispersive spectroscopy indicates the presence of Zn and S.

Conclusions

To summarize, a new route for the preparation of semiconductor Q-particles has been presented. Optical spectroscopy and TEM indicate that the particles are sufficiently small to exhibit quantum optical characteristics. Importantly, the pore sizes of the sol-gel-derived films, which are controlled by the aging time of the sol, control particle size. In addition, the thin composite films are stable and transparent and do not scatter a significant fraction of incident light. Finally, thermal annealing of the films results in semiconductor particle growth. The use of controlled pore size thin-film hosts as templates for controlling particle growth is a general strategy for the preparation of nanocomposites with tailored properties. Details of the preparation and characterization of PbS, Ag, and Au Q-particles will be presented separately.[36]

Acknowledgment. We thank Ms. Carol Ashley for preparing the sol-gel solutions. TEM facilities were provided by the UNM Department of Geology Electron Microbeam Analysis Facility. This work was funded by the Department of Energy, Division of Basic Energy Sciences, and the UNM/NSF Center for Micro-Engineered Ceramics, a collaborative effort supported by NSF (CDR-8800352), Los Alamos and Sandia National Laboratories, the New Mexico Research and Development Institute, and the ceramics industry.

References and Notes

(1) Rossetti, R.; Hull, R.; Gibson, J. M.; Brus, L. E. *J. Chem. Phys.* **1985**, *82*, 552.
(2) Wang, Y.; Herron, N. *J. Phys. Chem.* **1991**, *95*, 525.
(3) Lippens, P. E.; Lannoo, M. *Phys. Rev. B* **1989**, *39*, 10935.
(4) Wang, Y.; Suna, A.; Mahler, W.; Kasowski, R. *J. Chem. Phys.* **1987**, *87*, 7315.
(5) Steigerwald, M. L.; Brus, L. E. *Acc. Chem. Res.* **1990**, *23*, 183.
(6) Steigerwald, L. M.; Brus, L. E. *Annu. Rev. Mater. Sci.* **1989**, *19*, 471.
(7) Alivisatos, A. P.; Harris, A. L.; Levinos, N. J.; Steigerwald, M. L.; Brus, L. E. *J. Chem. Phys.* **1988**, *89*, 4001.
(8) Herron, N. In *Materials for Nonlinear Optics: Chemical Perspectives*; Mardar, S. R., Sohn, J. E., Stucky, G. D., Eds.; ACS Symposium Series 455; American Chemical Society: Washington, DC, 1990; p 582.
(9) Brus, L. E. *J. Chem. Phys.* **1984**, *80*, 4403.
(10) Henglein, A. *Chem. Rev.* **1989**, *89*, 1861.
(11) Meyer, M.; Wallberg, C.; Kurihara, K.; Fendler, J. H. *J. Chem. Soc., Chem. Commun.* **1984**, *2*, 90.
(12) Fendler, J. H. *Chem. Rev.* **1987**, *87*, 877.
(13) Lianos, P.; Thomas, J. K. *J. Colloid Surf. Soc.* **1986**, *117*, 505.
(14) Daunhauser, T.; O'Neal, M.; Johansson, K.; Witten, D.; McLendon, G. *J. Phys. Chem.* **1986**, *90*, 854.
(15) Wang, Y.; Mahler, W. *Opt. Commun.* **1987**, *61*, 233.
(16) Wang, Y.; Herron, N. *J. Phys. Chem.* **1987**, *91*, 257.
(17) Fojitk, A.; Weller, H.; Koch, U.; Henglein, A. *Ber. Bunsen-Ges. Phys. Chem.* **1984**, *88*, 969.
(18) Coffer, J. L.; Beauchamp, G.; Zerda, T. W. *J. Non-Cryst. Solids*, in press.
(19) Yamamoto, T.; Taniguchi, A.; Dev, S.; Kubota, E.; Osakada, K.; Kubota, K. *Colloid Polym. Sci.* **1991**, *269*, 969.
(20) Herron, N.; Wang, Y.; Eddy, M. M.; Stucky, G. D.; Cox, D. E.; Moller, K.; Bein, T. *J. Am. Chem. Soc.* **1989**, *111*, 530.
(21) Spanhel, L.; Schmidt, H.; Uhrig, A.; Klingshirn, C. In *Better Ceramics Through Chemistry V*; Hampden-Smith, M. J., Klemperer, W. G., Brinker, C. J., Eds.; Materials Research Society: Pittsburgh, PA, to be published.
(22) Gacoin, T.; Boilot, J. P.; Chaput, F.; Lecomte, A. In *Better Ceramics Through Chemistry V*; Hampden-Smith, M. J., Klemperer, W. G., Brinker, C. J., Eds.; Materials Research Society: Pittsburgh, PA, to be published.
(23) Nogami, M.; Watabe, M.; Nagasaka, K. In *Sol-Gel Optics*; Mackenzie, J. D., Ulrich, D. R., Eds.; S.P.I.E.: San Diego, 1990; Vol. 1328, p 119.
(24) Cummins, C. C.; Schrock, R. R.; Cohen, R. E. *Chem. Mater.* **1992**, *4*, 27.
(25) Chandler, R. R.; Coffer, J. L.; Gutsche, C. D.; Alam, I.; Yang, H.; Pinizzotto, R. F. In *Better Ceramics Through Chemistry V*; Hampden-Smith, M. J., Klemperer, W. G., Brinker, C. J., Eds.; Materials Research Society: Pittsburgh, PA, to be published.
(26) Roy, R.; Komarneni, S.; Roy, D. M. *Better Ceramics Through Chemistry I*; Brinker, C. J., Clark, D. E., Ulrich, D. R., Eds.; Elsevier: New York, 1984; pp 347-359.
(27) Rajh, T.; Vucemilovic, M. I.; Dimitrijevic, N. M.; Micic, O. I. *Chem. Phys. Lett.* **1988**, *143*, 305.
(28) Kuczynski, J.; Thomas, J. K. *J. Phys. Chem.* **1985**, *89*, 2720.
(29) Brinker, C. J.; Mukherjee, S. P. *J. Mater. Sci.* **1981**, *16*, 1980.
(30) Brinker, C. J.; Scherer, G. W. *Sol-Gel Science*; Academic Press: San Diego, 1990; pp 807-808.
(31) Brinker, C. J.; Frye, G. C.; Hurd, A. J.; Ashely, C. S. *Thin Solid Films* **1991**, *201*, 97.
(32) Glaves, C. L.; Frye, G. C.; Smith, D. M.; Brinker, C. J.; Datye, A.; Ricco, A. J.; Martin, S. J. *Langmuir* **1989**, *5*, 459.
(33) *Powder Diffraction File Alphabetical Index, Inorganic Phases*; McClune, W. F., Ed.; JCPDS Internation Center for Diffraction Data: Swarthmore, 1988; Card No. 5-0566.
(34) Absorption thresholds were taken as the wavelength corresponding to the discontinuity in the slope of the scale-expanded optical absorption spectra. As in previous studies, there is a degree of arbitrariness in this approach.
(35) Reference 30, Chapter 6.
(36) Zhang, Y.; Brinker, C. J.; Crooks, R. M. Manuscript in preparation.

Electron Emission Mechanism for Impact of C_N^- and Si_N^- Clusters

Pamela M. St. John, Chahan Yeretzian, and Robert L. Whetten*

Department of Chemistry and Biochemistry, University of California, Los Angeles, California 90024-1569
(Received: August 24, 1992)

Surface collisions of negatively charged atomic clusters C_N^- and Si_N^-, $N < 15$, have been investigated by time-of-flight methods. At low impact velocities (<10 km/s), the intact scattered ion and its charged fragments are clearly observed, along with ejected electrons. The time profile for the electron is broad and asymmetric, proving that it arises from *delayed emission from the intact scattered negative ion.* This provides a simple explanation for the low-energy emission found by Achiba and co-workers which they attribute to cluster electronic excitation. The relative yield of ions and electrons suggests that fragmentation and electron emission are competing processes for cooling the hot scattered ion.

Introduction

In a series of recent reports, Achiba and co-workers have documented an electron emission process that occurs when certain negatively charged clusters A_N^- (A = C, Si) collide with a solid surface.[1-3] This process is characterized by a threshold at low impact energy and a maximum yield at a velocity well below the threshold velocity for secondary particle emission from the solid; the yield is also complementary to the surface current. The threshold energy appears to be correlated with the electron affinity of the cluster, and it was suggested that the yield may be correlated to cluster structure as well. The mechanism for this process has not been clarified, although Moriwaki et al.[2] have proposed that impact induces electron excitation of the cluster, resulting in prompt emission to vacuum, as illustrated in Figure 1 (upper).

Concurrently, we have investigated the scattering of various charged cluster from solid surfaces.[4-10] Among the observables in such experiments is the identity (mass) and time of flight of the scattered charged particles, including electrons. In the case of C_{60}^- and several Si_N^-, we have described how electron emission appears to compete directly with detection of the scattered parent

0022-3654/92/2096-9100$03.00/0